Tuning microcapsules surface morphology using blends of homo- and copolymers of PLGA and PLGA-PEG

Emilia Pisani,[ab] Catherine Ringard,[ab] Valérie Nicolas,[c] Elie Raphaël,[d] Véronique Rosilio,[ab] Laurence Moine,[ab] Elias Fattal[ab] and Nicolas Tsapis*[ab]

Received 30th January 2009, Accepted 5th June 2009
First published as an Advance Article on the web 8th July 2009
DOI: 10.1039/b902042j

We modulate precisely the surface morphology of polymer microcapsules containing perfluorooctyl bromide prepared by the solvent-evaporation technique by varying the percentage of PLGA-PEG copolymer in the formulation. As copolymer percentage increases, protrusions start to appear, become more numerous and finally fuse to yield sponge-like capsules. It has been postulated that the shell morphology arises from an interfacial tension instability. We show here that if an interfacial tension instability develops, it happens during the final step of polymer desolvation, when the interface is no longer fluid and interfacial tension changes cannot be monitored. The formation of protrusions occurs in order to accommodate all the PEG chains of the copolymer in a hydrophilic environment, since PEG and PLGA moieties are not miscible in the solid state.

Introduction

Although colloids of non-spherical or anisotropic shapes exist in nature, precise control of colloid shape has attracted a lot of attention in recent decades.[1] Recent advances in micro- and nanoparticle synthesis focus on producing non-spherical particles and anisotropic particles for photonic crystal applications[2,3] or hollow particles for drug delivery purposes.[4–6] In drug delivery applications, particle morphology may influence either delivery properties[4,7,8] (as it is the case for lung delivery) or drug release profiles.[9,10] Among the various existing strategies to modulate particle morphology and drug release, the most commonly used consist in blending a hydrophobic homopolymer with an amphiphilic copolymer containing a polyethylene glycol moiety. In particular, using the common solvent emulsion–evaporation technique, Gref *et al.*[9] have shown that replacing hydrophobic poly(lactide) (PLA) by amphiphilic poly(lactide)–polyethylene glycol (PLA-PEG) led to sponge-like microspheres with faster drug release. Similar sponge morphologies were observed by Zhu and Hayward[11] with polystyrene–polyethylene glycol amphiphilic copolymers. They attributed these structural changes to interfacial instabilities at the emulsion droplet interface during solvent evaporation.

In the present study, we have investigated the possibility to apply the previous strategy to modify the surface morphology of capsules prepared by a modified solvent emulsion–evaporation method, devoted to medical imaging coupled to drug delivery.[12] The original capsules consist of a shell of poly(lacide-*co*-glycolide) (PLGA) surrounding a liquid core of perfluorooctyl bromide (PFOB). PLGA was progressively replaced by poly-(lacide-*co*-glycolide)-polyethylene glycol (PLGA-PEG) and the resulting capsule surface morphologies were imaged by microscopic techniques. Capsules were also characterized in terms of size and specific surface area as a function of PLGA-PEG percentage. In addition, interfacial tension measurements were performed to gain more insight on how copolymers organize at microcapsule surface.

Materials and methods

Materials

Poly(lactide-*co*-glycolide) 50:50 Resomer RG502 (MW = 12000 g/mol) and poly(ethylene glycol)-poly(DL-lactide-*co*-glycolide) 50:50 Resomer PEG type RGP d 50105 (MW = 50000 g/mol) (diblock, 10% PEG with 5000 Dalton) were obtained from Boehringer-Ingelheim (Germany). Sodium cholate (SC), and Nile Red were purchased from Sigma-Aldrich. Perfluorooctyl bromide (PFOB) was from Fluorochem (UK). Dichloromethane RPE-ACS 99.5% was obtained from Carlo Erba Reactifs (France). The ultrapure water was produced by a Millipore Synergy 185 apparatus coupled with a RiOs5™ (Millipore, France), with a resistivity of 18.2 MΩ cm.

Sample preparation

100 mg of polymer (PLGA and/or PLGA-PEG) was dissolved into 4 ml dichloromethane along with 60 μL of PFOB and placed in a thermostated bath maintained at 20 °C to ensure full miscibility of PFOB with dichloromethane at this concentration. The organic solution was then emulsified into 20 mL of sodium cholate aqueous solution using an Ultra-turrax T25 (IKA) operating with a SN25-10G dispersing tool at a velocity of 8000 rpm. Emulsification was performed in a 50 mL beaker placed over ice for 2 min. Dichloromethane was then evaporated by magnetic stirring for about 3 h at 300 rpm in a thermostated bath

[a]*Univ. Paris Sud, UMR CNRS 8612, IFR 141-ITFM, Faculté de Pharmacie, 5 Rue Jean-Baptiste Clément, 92296 Châtenay-Malabry, France. E-mail: nicolas.tsapis@u-psud.fr; Fax: +33146619334*
[b]*CNRS, UMR 8612, IFR 141-ITFM, Faculté de Pharmacie, Châtenay-Malabry, France*
[c]*IFR 141-ITFM, Plateforme Imagerie Cellulaire, Châtenay-Malabry*
[d]*UMR CNRS Gulliver 7083, ESPCI, Paris, France*

(20 °C) or in a rotary evaporator under reduced pressure for about 1 h at 700 rpm (room temperature). For fluorescent or confocal microscopy, Nile Red was added to the organic solution prior to emulsification to label the polymer phase. Typically, about 100 μl of a concentrated Nile Red solution (0.057 mg/ml in dichloromethane) were added.

Granulometry

Size measurements on microcapsules were performed using a LS230 Coulter-Beckmann granulometer based on laser diffraction. Drops of the capsule suspension were added to water in the measurement cuvette. Measurements were performed in triplicate.

Optical and fluorescence microscopy

Samples in water were placed between glass slides and observed with a Leitz Diaplan microscope equipped with a Coolsnap ES camera (Roper Scientific). Fluorescent samples dyed with Nile Red were excited at 543 nm and observed at 560 nm (long-pass filter).

Confocal microscopy

Glass slides were examined with a Zeiss LSM-510 confocal scanning laser microscope equipped with a 1 mW helium–neon laser, using a Plan Apochromat 63X objective (NA 1.40, oil immersion). Red fluorescence was observed with a long-pass 560 nm emission filter under 543 nm laser illumination. The pinhole diameter was set at 71 μm. Stacks of images were collected every 0.42 μm along the *z*-axis. The images presented below correspond to slices obtained in the equatorial plane of the capsules.

Scanning electron microscopy

Scanning Electron Microscopy (SEM) was performed using a LEO 1530 (LEO Electron Microscopy Inc, Thornwood, NY) operating between 1 kV and 3 kV with a filament current of about 0.5 mA. Sample suspensions were deposited on carbon conductive double-sided tape (Euromedex, France) and dried at room temperature. They were coated with a palladium-platinum layer of about 4 nm using a Cressington sputter-coater 208HR with a rotary-planetary-tilt stage, equipped with a MTM-20 thickness controller. Before imaging, particles were washed either by centrifugation or dialysis to remove the excess of surfactant that reduces the quality of images.

Interfacial tension measurements

Interfacial tension measurements were performed by the pendant drop method, using the Drop Shape Analysis System DSA 100 (Krüss, Germany). Dichloromethane drops containing the polymer at 25 mg/mL or 100 mg/mL with different weight proportions of PLGA-PEG were formed in pure water or an aqueous solution of sodium cholate (1.5% w/v). The interfacial tension values were determined from at least ten independently formed drops. The volume of the drops was maintained constant and the interfacial tension was monitored until a constant value was obtained (generally in less than 3 min). The temperature of experiments was 20 ± 1 °C. The experimental uncertainty was estimated to be smaller than 0.2 mN/m.

Specific surface area measurements

The specific surface area was measured from the Brunauer-Emmett-Teller (BET) isotherms of nitrogen adsorption and desorption using a SA3100 (Beckmann-Coulter). Microcapsules were washed twice by centrifugation to remove the excess of surfactant, frozen at −20 °C and freeze-dried for 48 h using a LYOVAC GT2 before measurements.

Results and discussion

The encapsulation of liquid perfluorooctyl bromide within a biodegradable[13] and biocompatible[14] polymeric shell of PLGA to develop an ultrasonic contrast agent candidate has been optimized and reported in detail in previous articles.[12,15,16] The method used to obtain microcapsules composed of a solid polymeric shell encapsulating a liquid perfluorooctyl bromide (PFOB) core is derived from the technique described by Loxley *et al.*[17] and used by many others since.[18–21] It is a modification of the commonly used emulsion–evaporation process. The organic phase is a mixture of PLGA, dichloromethane (a low-boiling good solvent for PLGA), and PFOB (a high-boiling very poor solvent for PLGA). Enough dichloromethane is present to ensure that PLGA is completely dissolved and that the liquid PFOB is fully miscible. The organic phase is then emulsified in an aqueous solution of surfactant, and the low-boiling solvent is evaporated. Evaporation allows gradual removal of the dichloromethane from the emulsion droplets. Since PFOB is very poorly miscible in dichloromethane, the droplet composition reaches quickly the binodal boundary and PFOB phase-separates into small droplets within the emulsion globules of polymer–dichloromethane. At the same time, due to the poor solubility of the polymer in PFOB, the dichloromethane phase becomes more and more concentrated in PLGA. When wetting conditions are optimal, the polymer–dichloromethane globule fully engulfs the PFOB droplet, leading to the desired capsule morphology. Further solvent removal causes the polymer to precipitate at the interface, forming a solid shell.[17] In a strategy to modify microcapsule surface morphology, PLGA was partially or totally replaced in the formulation by PLGA-PEG.

Bright field and fluorescence microscopy observations reveal that the PFOB core is preserved independently of the percentage of PLGA-PEG (Fig. 1). The water–polymer interface appears rather rough for 5% PLGA-PEG and almost fuzzy for 100% PLGA-PEG. In addition, the capsule thickness is not as homogeneous as it is for PLGA capsules, with obvious differences in fluorescence levels within the shell (Fig. 1). Theses morphology modifications are associated with an increase of the capsule size. Size measurements show that the median diameter (D_{50}) of the microcapsules increases from 6 μm for pure PLGA to 13 μm for pure PLGA-PEG (Fig. 2). Fig. 3 presents microscopy images of typical capsules for different PLGA-PEG percentages. Bright field microscopy suggests that the initially smooth surface becomes 'spiky' with 5% and 10% PLGA-PEG and 'hairy' from 20% to 100% PLGA-PEG. These observations are confirmed by confocal slices of capsules taken in their equatorial plane, where

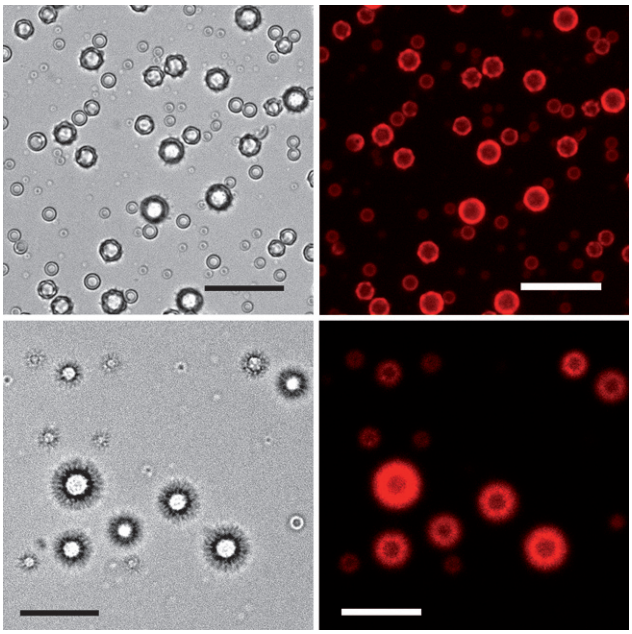

Fig. 1 Microscopy images of typical microcapsule suspensions (left: bright field, right: fluorescence) obtained by replacing 5% (w/w) (top), or 100% (w/w) (bottom) of PLGA by PLGA-PEG. Scale bars represent 20 μm.

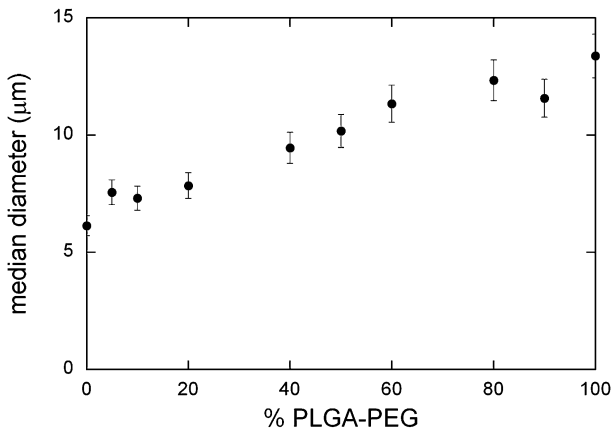

Fig. 2 Median diameter (D_{50}) of microcapsules as a function of PLGA-PEG percentage.

the red fluorescence arises from the polymer. On one hand, the core–shell morphology is preserved with a smooth interface between the PFOB core and the polymer independently of the PLGA-PEG proportion. In addition, the PFOB core size seems to remain identical. On the other hand, the water polymer interface is fuzzy, with polymer protrusions extending towards the exterior of the capsule. SEM images further confirm the existence of protrusions from 5 to 20% of PLGA-PEG. For larger PLGA-PEG proportions, protrusions seem to have fused into polymer sheets, forming a shell of increasing porosity until it appears almost sponge-like from 60 to 100% PLGA-PEG. The protrusions present on the shell explain the observed size increase, since the same polymer mass is distributed in a spiky or spongy shell that is thicker than a dense one. We have evaluated the effect of the evaporation speed: no morphology differences were observed between microcapsules obtained after evaporation under reduced pressure or atmospheric pressure. They more probably depend on the organization of the polymer at the interface related to geometrical or thermodynamical constraints.

Porous microspheres have been obtained with PLA-PEG by Gref *et al.* using the same process, but the influence of the percentage of PLA-PEG on microsphere morphology was not investigated.[9] Fig. 4 presents bright field and confocal microscopy images obtained for microspheres prepared without PFOB. As with PFOB microcapsules, the water–polymer interface becomes rough and spiky when 5% PLGA is replaced by PLGA-PEG. For larger proportions of PLGA-PEG, the water–polymer interface is 'hairy', and confocal slices indeed confirm the porosity of the microspheres. SEM images are very similar to those obtained without PFOB (not shown here). Since similar morphologies were obtained without PFOB in the formulation, it demonstrates that microcapsule structuration does not arise from PFOB/PLGA–PEG interactions but more likely from the behavior of the PEGylated polymer at the dichloromethane–water interface, as suggested by Gref *et al.*[9] Zhu and Hayward[11] have proposed that the protrusions observed using polystyrene–PEG copolymers arise from an interfacial tension instability. To observe and study this instability, we have investigated the morphology formation during the solvent evaporation process. After emulsification, the emulsion was collected every 15 min and observed with bright field and fluorescence microscopy. During the first 2.5 h of evaporation, no differences could be observed between formulations obtained with different proportions of PLGA-PEG. At the end of the first hour of evaporation, independently of the PLGA-PEG proportion, a PFOB droplet is visible within the emulsion globules. The PFOB droplet volume increases whereas the water–dichloromethane interface remains smooth for another 1.5 h. Then, as the polymer fully desolvates, the microcapsule shell becomes structured depending of the PLGA-PEG proportions (Fig. 5). For 5% PLGA-PEG, the water–dichloromethane interface becomes rough and small polymer protrusions appear. For 100% PLGA-PEG, the polymer shell becomes fuzzier as solvent evaporates, finally taking on its porous structure. These observations show that if an interfacial tension instability develops, it has to happen during the final step of desolvation of the polymer. This instability would then be frozen by the polymer precipitation, leading to different morphologies observed depending on the PLGA-PEG proportion.

Measuring the interfacial tension throughout solvent evaporation is rather difficult, since polymer precipitation occurs almost immediately after protrusions appear. Interfacial tensions were measured for two polymer concentrations as a function of PLGA-PEG percentage: 25 and 100 mg/mL. The first concentration corresponds to the polymer concentration in dichloromethane just before emulsification. The second one corresponds to the highest concentration we were able to work with, without observing polymer precipitation as soon as in contact with the aqueous solution. This high concentration would account for the changes occurring during polymer desolvation.

The interfacial tension behavior is quite different at the dichloromethane–water interface and at the dichloromethane–sodium cholate solution interface (Fig. 6). At the dichloromethane–water interface, the interfacial tension decreases abruptly by 5 mN/m as soon as 5% PLGA-PEG is added to

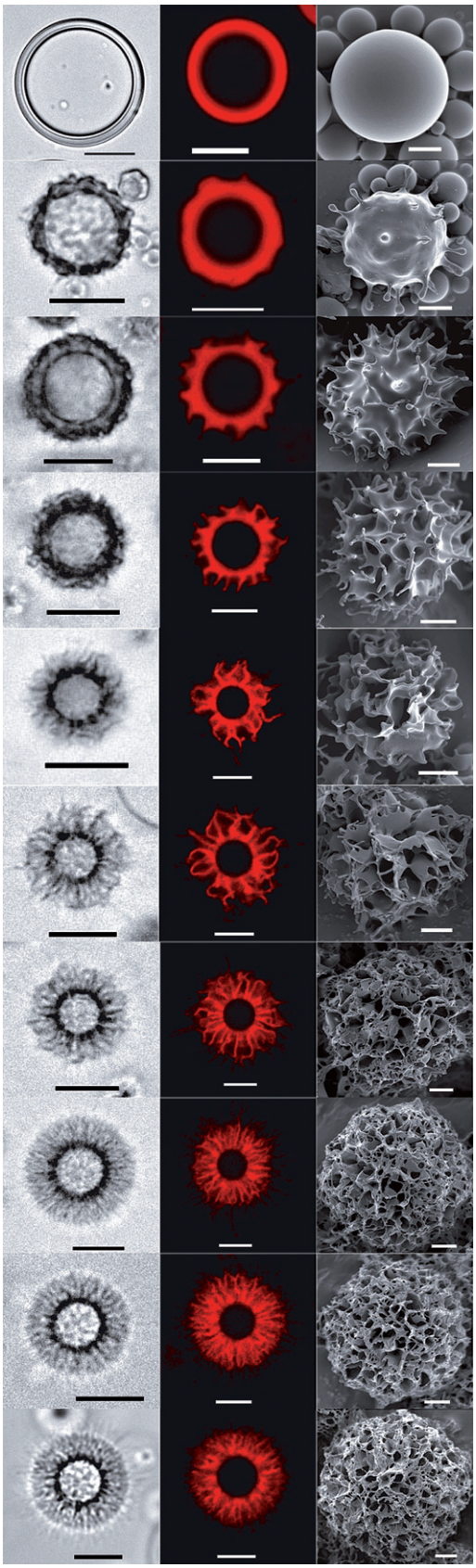

Fig. 3 Bright field (left), confocal (center) and SEM (right) images of a typical microcapsule obtained with different percentages of PLGA-PEG: 0, 5, 10, 20, 40, 50, 60, 80, 90 and 100% from top to bottom Scale bars represent 10 μm (bright field), 5 μm (confocal microscopy) and 2 μm (SEM).

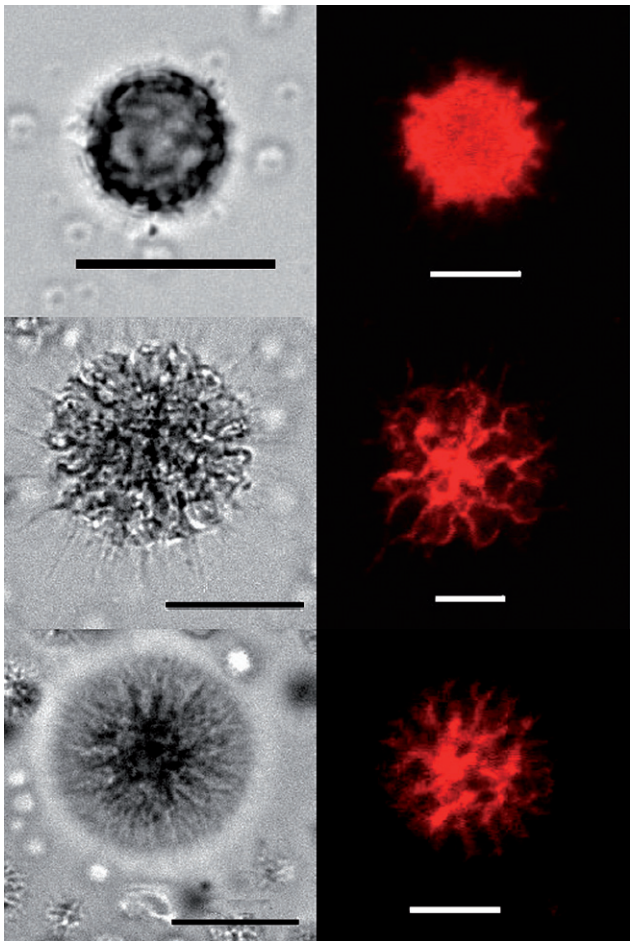

Fig. 4 Bright field (left) and confocal microscopy (right) images of typical microspheres obtained with different percentages of PLGA-PEG: 5, 50, and 100% from top to bottom. Scale bars represent 10 μm (bright field) and 5 μm (confocal microscopy).

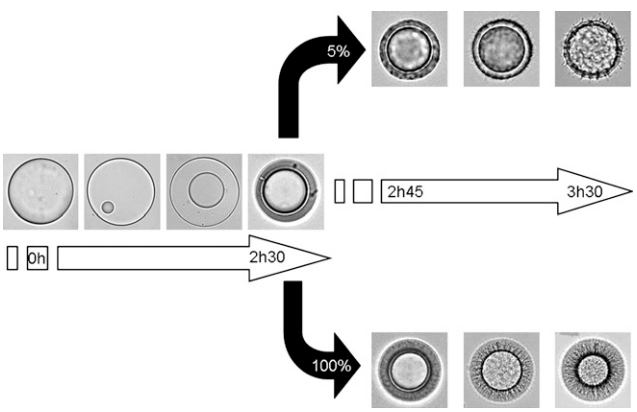

Fig. 5 Bright field images of the different steps of the evaporation process. The interface structuration, which is dependent of the percentage of PLGA-PEG, only happens during the last hour of evaporation.

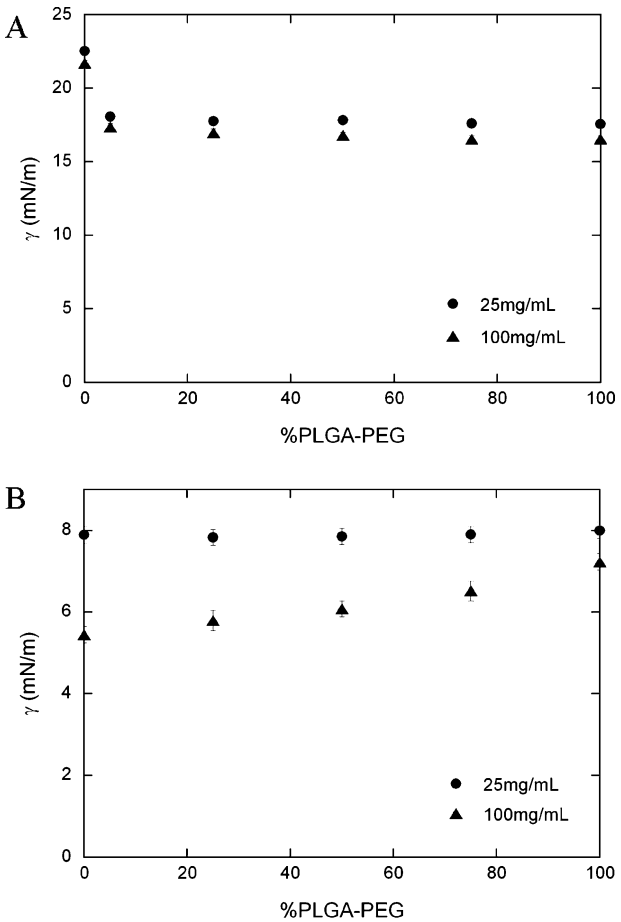

Fig. 6 Interfacial tension as a function of the weight percentage of PLGA-PEG for two different concentrations of polymer in dichloromethane 25 and 100 mg/mL. The top graphic (A) corresponds to the dichloromethane–water interface, whereas the bottom graphic (B) corresponds to the dichloromethane–sodium cholate solution interface.

PLGA. This decrease is independent of the polymer concentration, although the interfacial tension is always about 1 mN/m higher for 25 mg/mL polymer concentration (Fig. 6). Then, as the PLGA-PEG percentage increases, the interfacial tension remains constant. At the dichloromethane–sodium cholate solution interface, for 25 mg/mL copolymer, the interfacial tension is fairly steady as a function of the percentage of PLGA-PEG around 8 mN/m. Conversely, for 100 mg/mL copolymer, the interfacial tension increases as a function of the percentage of PLGA-PEG from about 5.4 mN/m to about 7.2 mN/m.

The dichloromethane–water interfacial tension is 28.2 mN/m. When PLGA is dissolved in the organic solvent, a lowering in the interfacial tension is observed, indicating the adsorption of the polymer at the solvent–water interface (Fig. 6, top). This lowering is limited ($\Delta\gamma$ is about 4 mN/m) and is almost identical whatever the concentration of the polymer (25 or 100 mg/ml). Obviously, at both concentrations, the critical aggregation concentration of the polymer is already reached. When 5% of PLGA-PEG is mixed with PLGA, an additional lowering in the interfacial tension is observed ($\Delta\gamma = 5$ mN/m). Interestingly, it is more the presence of PLGA-PEG at the interface which seems responsible for this lowering than the extent of PLGA-PEG content in the mixture. Indeed, the lowering in the interfacial tension is identical when the organic solvent contains PLGA-PEG only. This indicates that the organization of PLGA-PEG molecules within the interfacial film does not change with PLGA-PEG concentration. When sodium cholate is added to the water phase, at the total polymer concentration of 25 mg/ml, the interfacial tension is lowered to $\gamma = 8$ mN/m. In a previous study, we showed that the interfacial tension of dichloromethane–sodium cholate solution was 8 mN/m.[16] With 25 mg/ml PLGA, it was lowered to 7 mN/m, which was an insignificant change. In these new experiments, the lowering of the interfacial tension due to the sodium cholate solution in the presence of PLGA was not even apparent. Obviously, sodium cholate adsorbs at the interface much more rapidly than PLGA and hinders the adsorption of the copolymer, whatever its composition, at short time-scales. However, when the total concentration of the copolymers is increased to 100 mg/ml, the interfacial tension is lowered to 5.5 mN/m in the presence of PLGA alone. At this polymer concentration, PLGA seems able to compete with sodium cholate for the interface or, at least, to interact with the surfactant monolayer. However, in the presence of increasing amounts of PLGA-PEG, the interfacial tension progressively increases and gets closer to that of the bare dichloromethane–sodium cholate solution interface. This would indicate that less copolymer is adsorbed at the interface, or that the organization of the adsorbed PLGA is altered in the presence of the PEG chains. Apparently, due to the PEG chain, PLGA-PEG, at high concentration in the organic phase, would be unable to organize as PLGA alone. In the microcapsules, since the copolymer is insoluble in PFOB, and the dichloromethane layer becomes thinner during solvent removal, steric interactions among the numerous PEG chains in the vicinity of the interface and the larger molecular weight of this copolymer would account for the partial diffusion of PLGA-PEG in the water phase, where more space is available. The PEG chain especially would favor protrusion of the copolymer at the interface. Instead of a mixed PLGA/PLGA-PEG/sodium cholate film, the interface would be mainly formed of sodium cholate molecules, the two copolymers chains possibly adsorbed in a loose sublayer. Together, these results clearly suggest that the surface morphology changes occur upon polymer desolvation when the interface becomes solid and interfacial tension measurements can no longer be performed.

The interface reorganisation could be explained as follows. It is well-known that dichloromethane is a better solvent for PEG than water,[22,23] explaining why functionalised PEG is usually isolated in dichloromethane from water-soluble impurities/reactants *via* dichloromethane–water liquid–liquid extractions. As long as there is enough dichloromethane in the medium to solubilise PEG chains, the copolymer remains in the bulk of the hydrophobic solvent. As the copolymer reaches its solubility limit in dichloromethane, it migrates to the interface and exposes PEG moieties towards the aqueous phase, since it becomes energetically more favorable than mixing PEG chains with PLGA in the solid state. In order to expose all the PEG chains into the aqueous environment, some interface must therefore be created. The interface creation is confirmed by specific surface area measurements (Fig. 7). As the percentage of PLGA-PEG increases, the specific surface area, which starts around 1 m^2/g, first increases slowly, then more steeply until it reaches

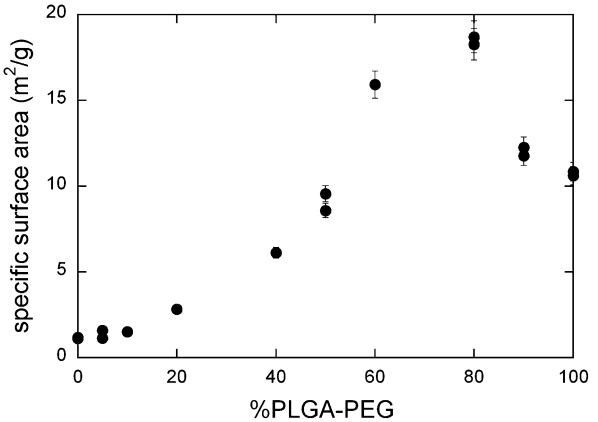

Fig. 7 Specific surface area as a function of the percentage of PLGA-PEG in the microcapsule formulation.

a maximum of about 20 m^2/g for 60–80% PLGA-PEG, and then decreases back to about 10 m^2/g. The specific surface area increase correlates well with microscopic observations of capsule morphology. The spiky protrusions present at low percentages of PLGA-PEG do not lead to a huge increase of interface area.

The higher the PLGA-PEG percentage, the more numerous the spiky protrusions and the larger the specific surface area. When protrusions become too numerous, they probably fuse during polymer desolvation and therefore lead to the observed decrease of specific surface area. The hypothesis of interface creation is further supported by SEM images obtained at low PLGA-PEG percentages (Fig. 3). Indeed at 5% PLGA-PEG, only the larger particles exhibit protrusions, whereas the smaller ones whose specific surface area is larger are smooth since they can accommodate easily all the PEG chains at their surface. The specific surface area (S_{sp}) of the microcapsule suspension is $S_{sp} = 6/D\rho$, where ρ is the density (1.5 g/cm^3),[15] giving $S_{sp} = 0.667$ m^2 g^{-1}. This theoretical value is of the order of the value 1.15 m^2 g^{-1} found experimentally. The difference probably arises from microcapsule polydispersity. For a typical preparation, the available surface is therefore $S_{sp} \times 0.18$ g = 0.12 m^2. According to Gref *et al.*, 2 nm^2 is the minimal area available for 5000 Da PEG chains.[24] It is therefore possible to accommodate up to $0.12 / 2 \times 10^{-18} = 6 \times 10^{16}$ chains at the surface of microcapsules. If the number of PEG chains is above this value, in order for all the hydrophilic chains to be exposed to the aqueous medium, surface is created, explaining the observed protrusions. The number of PEG chains corresponding to 5% PLGA-PEG by weight in the preparation can be calculated:

$$N_{PEG5} = \frac{0.005}{50000} \times N_{Avogadro} = 6 \times 10^{16}$$

The fact that the above numbers coincide explains why 5% PLGA-PEG is approximately the concentration at which protrusions start to appear.

Conclusion

We have shown that it is possible to tune precisely the surface morphology of polymer microcapsules of perfluorooctyl bromide by varying the percentage of PLGA-PEG copolymer in the formulation. At low copolymer percentages, protrusions start to appear. As copolymer percentage increases, protrusions become more numerous until they fuse to yield a sponge-like shell. Zhu and Hayward[11] proposed that these protrusions arise from an interfacial tension instability. However, we found that it is not possible to experimentally measure an interfacial tension change as the instability develops, since it occurs when the interface becomes solid during the last step of polymer desolvation. We propose a microscopic mechanism for the development of this instability based on PEG solubility switch as dichloromethane evaporates. As long as there is enough dichloromethane to solubilise PEG chains, the copolymer remains in the bulk. When the copolymer reaches its solubility limit in dichloromethane, it migrates to the interface to expose PEG moieties towards the aqueous phase, since it costs less energy than if PEG was mixed with PLGA in the solid state. In order to expose all the PEG chains to the aqueous environment, some interface must therefore be created, explaining the observed protrusions.

Acknowledgements

The authors acknowledge financial support from the Agence Nationale de la Recherche (ANR ACUVA NT05-3_42548), in particular for the E. Pisani fellowship. The authors would like to thank A. Allavena-Valette (ICMPE, Thiais) for access to the SEM facility, and M. Deyme, R. Gref, N. Huang, J. P. Michel and J. Nicolas for stimulating discussions.

References

1 S. C. Glotzer and M. J. Solomon, *Nat. Mater.*, 2007, **6**(7), 557.
2 V. N. Manoharan, M. T. Elsesser and D. J. Pine, *Science*, 2003, **301**(5632), 483–487.
3 D. Zerrouki, J. Baudry, D. Pine, P. Chaikin and J. Bibette, *Nature*, 2008, **455**(7211), 380–382.
4 D. A. Edwards, J. Hanes, G. Caponetti, J. Hrkach, A. BenJebria, M. L. Eskew, J. Mintzes, D. Deaver, N. Lotan and R. Langer, *Science*, 1997, **276**(5320), 1868–1871.
5 N. Tsapis, D. Bennett, B. Jackson, D. A. Weitz and D. A. Edwards, *Proc. Natl. Acad. Sci. U. S. A.*, 2002, **99**(19), 12001.
6 G. De Rosa, F. Quaglia, A. Bochot, F. Ungaro and E. Fattal, *Biomacromolecules*, 2003, **4**(3), 529–536.
7 N. Tsapis, D. Bennett, K. O'Driscoll, K. Shea, M. M. Lipp, K. Fu, R. W. Clarke, D. Deaver, D. Yamins, J. Wright, C. A. Peloquin, D. A. Weitz and D. A. Edwards, *Tuberculosis*, 2003, **83**(6), 379–385.
8 C. Gervelas, A. L. Serandour, S. Geiger, G. Grillon, P. Fritsch, C. Taulelle, B. Le Gall, H. Benech, J. R. Deverre, E. Fattal and N. Tsapis, *J. Controlled Release*, 2007, **118**(1), 78.
9 R. Gref, P. Quellec, A. Sanchez, P. Calvo, E. Dellacherie and M. J. Alonso, *Eur. J. Pharm. Biopharm.*, 2001, **51**(2), 111.
10 A. L. G. dos Santos, A. Bochot, A. Doyle, N. Tsapis, J. Siepmann, F. Siepmann, J. Schmaler, M. Besnard, F. Behar-Cohen and E. Fattal, *J. Controlled Release*, 2006, **112**(3), 369.
11 J. Zhu and R. C. Hayward, *Angew. Chem., Int. Ed.*, 2008, **47**(11), 2113.
12 E. Pisani, N. Tsapis, B. Galaz, M. Santin, R. Berti, N. Taulier, E. Kurtisovski, O. Lucidarme, M. Ourevitch, B. T. Doan, J. C. Beloeil, B. Gillet, W. Urbach, S. L. Bridal and E. Fattal, *Adv. Funct. Mater.*, 2008, **18**, 2963.
13 A. M. Reed and D. K. Gilding, *Polymer*, 1981, **22**(4), 494–498.
14 K. Yamaguchi and J. M. Anderson, *J. Controlled Release*, 1993, **24**(1–3), 81.
15 E. Pisani, N. Tsapis, J. Paris, V. Nicolas, L. Cattel and E. Fattal, *Langmuir*, 2006, **22**(9), 4397–4402.

16 E. Pisani, E. Fattal, J. Paris, C. Ringard, V. Rosilio and N. Tsapis, *J. Colloid Interface Sci.*, 2008, **326**(1), 66.
17 A. Loxley and B. Vincent, *J. Colloid Interface Sci.*, 1998, **208**(1), 49.
18 R. Atkin, P. Davies, J. Hardy and B. Vincent, *Macromolecules*, 2004, **37**(21), 7979–7985.
19 P. J. Dowding, R. Atkin, B. Vincent and P. Bouillot, *Langmuir*, 2004, **20**(26), 11374–11379.
20 P. J. Dowding, R. Atkin, B. Vincent and P. Bouillot, *Langmuir*, 2005, **21**(12), 5278–5284.
21 F. M. Lavergne, D. Cot and F. Ganachaud, *Langmuir*, 2007, **23**(12), 6744–6753.
22 K. Tomaszewski, A. Szymanski and Z. Lukaszewski, *Talanta*, 1999, **50**(2), 299–306.
23 A. Malzert-Freon, J. P. Benoit and F. Boury, *Eur. J. Pharm. Biopharm.*, 2008, **69**(3), 835.
24 R. Gref, M. Luck, P. Quellec, M. Marchand, E. Dellacherie, S. Harnisch, T. Blunk and R. H. Muller, *Colloids Surf., B*, 2000, **18**(3–4), 301.

